RJC

RASĀYAN *J. Chem.*
Vol. 15 | No. 4 |2901-2907| October - December | 2022
ISSN: 0974-1496 | e-ISSN: 0976-0083 | CODEN: RJCABP
http://www.rasayanjournal.com
http://www.rasayanjournal.co.in

EFFECT OF COBALT DOPING AND ANNEALING ON PROPERTIES OF MANGANESE OXIDE THIN FILMS PREPARED USING JET NEBULIZER SPRAY PYROLYSIS TECHNIQUE

S. Saranya[1], N. Sethupathi[1,✉] and P. Mahalingam[2]

[1]Department of Physics, ArignarAnna Government Arts College, Namakkal-637002, Tamilnadu, India

[2]Department of Chemistry, ArignarAnna Government Arts College, Namakkal-637002, Tamilnadu, India

✉Corresponding Author: sethupathi2011@gmail.com

ABSTRACT

The controlled deposition and post-deposition treatments are fundamental steps in the synthesis of thin films in the range of nanometer to several micrometers in thickness for various applications. Because the uniform coating of nano-particles of doped metal oxide modifies the properties of metal oxide, thin films of cobalt-doped manganese oxide are prepared using the Jet nebulizer spray pyrolysis procedure at a temperature of 300°C in this study. The thin films are annealed in an air environment for two hours at various temperatures, including 350°C, 450°C, and 550°C. Cobalt thin films were produced and annealed for two hours at 550 °C in the air before being tested. The effect of annealing temperature and atomic percentage content of dopant cobalt in manganese oxide thin film on their properties were characterized by XRD, photoluminescence spectroscopy, UV-vis spectroscopic technique, scanning electron microscopy, and EDX. The characterization of the thin film reveals that these thin films are made up of uniformly coated doped metal oxide particles with (002) plan as a preferential orientation of crystal growth and band gap energy in the span of 2.5 -1.65 eV. The sensing property of the thin films towards ethanol was also characterized.

Keywords: Metal Oxide Thin Films, Spray Pyrolysis, Temperature, Composition, Ethanol Sensing.

RASĀYAN*J. Chem.*, Vol. 15, No.4, 2022

INTRODUCTION

Researchers show attention to metal oxide nanoparticles due to their optical, magnetic, and electrical properties. These metal oxides in their nano size exhibit different properties from their bulk material.[1] These peculiar properties of metal oxide nanoparticles induce researchers to employ transition metal oxides in their nano form for various potential applications like gas sensors, optoelectronic devices, and photovoltaic solar cells.[2-4]Though many transition metal oxides are available, manganese oxide is one of the considerable materials because, manganese oxides exist in various forms due to their variable oxidation state and also, exhibit high intrinsic movement of Mn.[5] Also, manganese oxides possess various crystalline phases and morphologies corresponding to MnO, MnO_2, Mn_2O_3, and Mn_3O_4. Manganese oxide thin films are utilized extensively in a wide range of applications, including sensors, solar cells, rechargeable batteries, catalysts, and magnetoelectronic devices, in addition to composites.[6] Since the thin film of metal oxide exhibits peculiar properties than the bulk material, researchers showed more interest in the preparation of a metal oxide thin film. Though several methods are available to prepare thin films because the spray pyrolysis technique creates nano-sized particles with controlled film thickness, is an excellent approach for thin film creation.[7-8] Doping manganese oxide thin films with transition metal are one of the efficient routes to improve their optical and electrical properties.[9] Even though intense research has been carried out on manganese oxide materials, manganese oxide and their doped thin films are limitedly studied.[10-14] Since spray pyrolysis produces good quality thin films, a modified form of it called the Jet nebulizer spray pyrolysis technique, which involves an effective atomization process to convert the solution into the mist is used to prepare thin films. The crystal structure and shape have a notable effect on the thin film's optical and electrical characteristics. The doping and annealing processes may be

http://doi.org/10.31788/RJC.2022.1547009

optimized to alter the characteristics of thin films obtained from their crystal structure and shape. The effect of doping and annealing on structural, optical, morphological, and sensing features of cobalt-doped manganese oxide thin films prepared by jet nebulizer spray pyrolysis are investigated in this study.

EXPERIMENTAL

This film is created by depositing thin films of cobalt-doped manganese oxide over a glass substrate. To eliminate any remaining impurities from the substrate, the glass plates are properly cleaned with double-distilled water. After this process, plates are immersed in a 2N nitric acid solution for the removal of oxide impurities on the surface of the glass substrate, again the substrate is washed with double distilled water and dried well.[15] To completely remove the impurities on the glass substrate, this process is repeated 3 times. Cobalt acetate ($Co(CH_3COO)_2$) and manganese acetate tetrahydrate $(CH_3COO)_2Mn.4H_2O$) are used to generate 0.2M stock solutions of the analytic grade chemicals. Appropriate quantities of the solutions have been mixed so as to get 2, 4, and 6 atomic percentages of cobalt in the film deposit. The mixtures are stirred well and then ultrasonicated for 10 minutes for homogenizing the solution. 8ml of the composition mixture is taken in the nebulizer and the top of the nebulizer is attached with a typically fabricated glass container tube. The bottom of the nebulizer is connected to a compressed air flow set with 4-atmosphere pressures. The compressed air converts the solution into mists. The mists are passed through the guiding glass tube to reach the well-cleaned glass substrate preheated at 300°C by an electrical heater. The mist which is deposited over the substrate undergoes pyrolytic decomposition to form metal oxide thin films at this temperature. The thin metal oxide coatings are annealed at 350, 450, and 550 degrees Celsius. XRD, PL, Uv-vis, SEM, and sensor systems are used to examine the influence of various annealing temperatures and compositions on cobalt-doped manganese oxide thin films in terms of structural, optical, morphological, and sensing features. Gas sensing system: It is etched tin oxide glass that is coated with cobalt-doped manganese oxide thin layers. Ohmic contacts are made using silver (Ag) paste. The sensor is placed in an electrically controlled furnace chamber maintained at the desired temperature (250 ºC). The ethanol and dry air are passed through the mass flow controller which can control the concentration of ethanol (100 ppm) in dry air for this study. The sensor is connected to a four-probe setup to measure the change in resistance. Based on the variation in resistance observed, sensing properties evolved.

RESULTS AND DISCUSSION

X-Ray Diffraction (XRD)

The effect of annealing temperature (350, 450, and 550°C) and dopant content (cobalt: 2, 4, and 6 at.%) on the crystalline nature of manganese oxide thin film are studied using the XRD technique. Figure-1a shows the usual XRD pattern of 4 at. percent (at. percent) cobalt-doped manganese oxide thin films annealed for two hours at 350°, 450°, and 550°C, as well as two and six at. Percent cobalt-doped manganese oxide thin films are annealed for two hours at the same temp (550°).

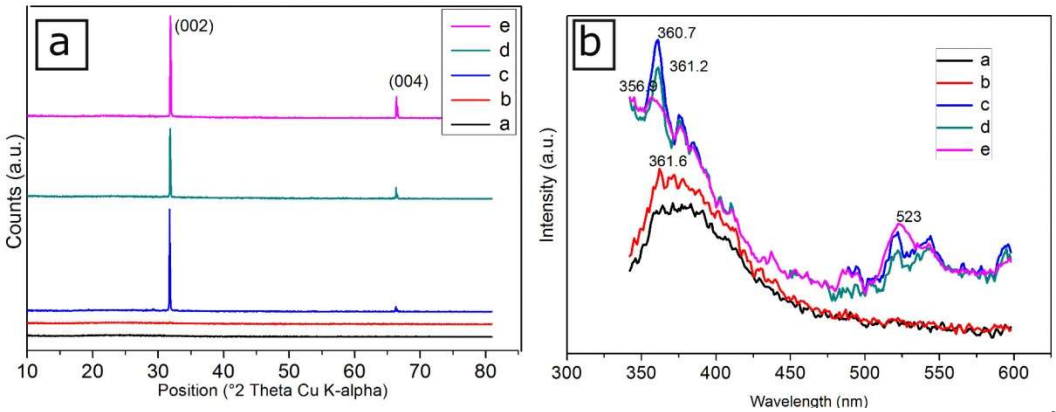

Fig.-1: (a) XRD and (b) PL pattern of 4 at. % cobalt doped manganese oxide thin film annealed at(a) 350^0C, (b) 450^0C and (c) 550^0C for 2hrs, (d) 2 at.% cobalt, (e) 6at. % cobalt doped manganese oxide thin films annealed at 550^0Cfor 2 hrs.

The absence of strong distinct peaks in the XRD pattern of the thin film that has been annealed at 350°C for two hours may be attributed to the amorphous state of metal oxide. The thin film annealed at 450°C for 2 hours shows a peak (2 thetas) at 31.77° but with low intensity. The peak formation at 31.77° (2 thetas) indicates the beginning of crystallization of the cobalt-doped manganese oxide on annealing at 450°C.[16]Increase in the temperature to 550°C and annealing for 2 hrs the particles of the thin film crystallize well is indicated by the intense peak at 31.87° and 66.37° corresponding to (200) and (400) planes. When the annealing temperature is raised to 550°C, the crystallization rate increases. In addition, the agglomeration of particles at higher temperatures might be linked to the growth of crystallites during annealing. Figure-1a depicts the XRD patterns of two-hour JNS-produced cobalt-doped manganese oxide thin films heated to 550°C. At 31.77° (2 thetas) there are strong and highly intense peaks that correspond to (200) and (400) planes, respectively, in the XRD pattern of thin films. There are no further distinct phases of Co that have been seen. The XRD pattern matches with the Hausmannite structure if the inconsistent poor intense peaks are discounted based on the disparity between nano and bulk crystalline particles.[17] Hausmannite structure is attributed to a complex mixture of Mn^{2+} and Mn^{3+} oxide.[18] The formula for the structure is $Mn^{2+}Mn_2^{3+}O_4$. Therefore, the prepared thin film particles can be considered to belong to the spinal group and form a tetragonal structure. The lattice parameters for the crystalline phase of the thin film are calculated using the equation (1).

$$\frac{1}{d_{hkl}^2} = \frac{h^2+k^2}{a^2} + \frac{l^2}{c^2} \quad (1)$$

Where a and c are lattice constants, d is the interplanar distance, and hkl is the Miller index. The values obtained of a, c, a/c, and unit cell size are 5.754Å, 9.330 Å, 1.6515, and 309.75 Å respectively. These numbers are quite close to what has been published.[19] The difference in ionic size between cobalt (II) (0.72Å) and manganese(II) (0.80Å), which vexes the electron cloud and creates a different environment, is responsible for a little deviation in lattice parameters. The crystallite size of the prepared cobalt-doped manganese oxide thin film is calculated using the Debye Scherrer equation (equation (2)).

$$D = \frac{k\lambda}{\beta cos\theta} \quad (2)$$

Since amorphous films annealed at 350 and 450 °C cannot be used to determine the crystallite size of the particles, the annealed at 550 °C thin films is used to do the calculation. As predicted, the average crystallite size of cobalt doped manganese oxide thin films was 32, 55, and 67 nm, according to the calculations. The JNS process may be used to manufacture cobalt-doped manganese oxide thin films with high crystallinity.

Photoluminescence (PL)

Photoluminescence spectrum (PL) was used to analyze the optical properties of prepared samples. Figure 1b shows the PL spectrum of cobalt doped manganese oxide thin films annealed at 350°C, 450°C, and 550°C, respectively. Thinned films that have been annealed at 350°C show a wider peak in the 350–400 nm wavelength range compared to those annealed at 450°C, which have an enhanced intensity in that range. In contrast, the 550°C-annealed thin film reveals a strong 360.7 nm peak and a peak in the 500-550 nm regions. When a thin film is annealed at 350 °C, surface imperfections or oxygen defects create broad peaks in the 350-400 nm range.[20] In the PL spectrum of a thin film that is annealed at 450°C, the band-to-band transition of metal oxides is fully evident. The band-to-band transition of metal oxides is clearly visible in the PL spectra of a thin film that was annealed at 450°C.[21] 550°C annealed thin film shows a peak in the near band edge transition at 360.7 nm.[22] The presence of an emission peak in the 500–550 nm region suggests that the samples have oxygen or crystal defects.[23] Increased annealing temperature leads to a rise in the intensity of the peaks, which may be attributed to the development of crystals in the thin films at extremely high temperatures. The photoluminescence spectrum of the cobalt-doped manganese oxide thin films exhibited in Image 1b is depicted in the figure after annealing at 550ºC for two hours(c,d,e). Cobalt-doped manganese oxide thin films with 2% cobalt had an absorbance peak at 361.2 nm, but those with 4% and 6% cobalt had an absorbance peak at a longer wavelength, respectively. In addition, when cobalt concentration rises, the peak's strength reduces at 360 nm and increases in the 475-550 nm region. This fact can be attributed to the increase in defects owing to an increase in cobalt

doping.[24] The cobalt can have good intercalation with the manganese oxide crystal lattice at low concentrations but at higher concentrations, it induces crystal defects.[25]

Scanning Electron Microscope (SEM)

Scanning electron microscopy has been utilized to assess the shape and particle size of the cobalt doped manganese oxide thin films. SEM is used to anneal manganese oxide thin films for two hours at 350, 450, and 550 degrees Celsius. There area uniform and smooth layer at both 350°C (Fig.-2a) and 450°C (Fig.-2b) thin film annealing conditions. However, particle formation is hardly found with these films which indicates that these films may be amorphous in nature. Whereas, the thin layer annealed at 550°C exhibits the crystalline nature of the particles with a compact, smooth, and uniform surface layer.

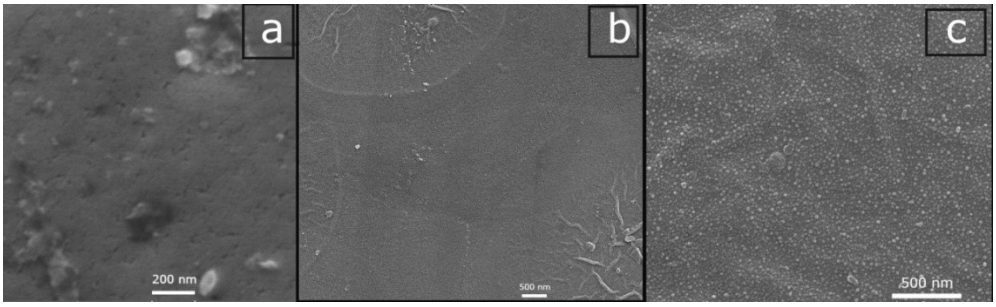

Fig.-2: SEM image of 4 at.% cobalt doped manganese oxide thin films annealed at (a) 350 °C (b) 450 °C and (c) 550 °C for 2 hrs.

The annealing temperature has a significant impact on the morphology of the thin film, as discussed in the preceding paragraphs. Moreover, the thin films are devoid of fractures and pinholes because the particles are firmly packed. In order to achieve a crystallized state, the film must be heated at 550ºC for 2 h at a rising temperature. The average particle size of thin film annealed at 550ºC for 2 h (Fig.-2c) is 60 nm, which could be correlated to the crystallite size obtained from XRD data of the film (55 nm). Since the crystallite size and the particle size are almost the same, the particles could be a perfect crystal and which is further supported by the sharp and intense peak observed in XRD.

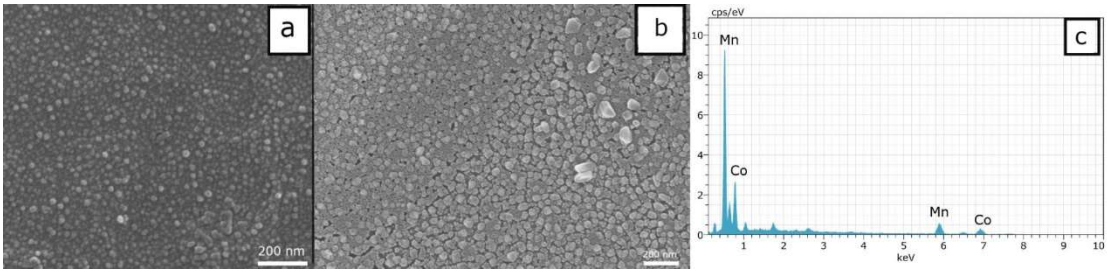

Fig.-3: SEM image of (a) 2 at.%, (b) 6 at.% cobalt doped manganese oxide thin films annealed at 550 °C for 2 hrs. (c) EDS spectrum of 4at.% cobalt doped manganese oxide thin films annealed at 550 °C for 2 hrs

Figure-3 shows JNS-prepared manganese oxide thin films with cobalt doping after two hours of annealing at 550°C. Figures 3a and 3b show SEM pictures of 2% and 6% of the samples, respectively. This type of manganese oxide thin film is composed of spherical particles of 40 nm in diameter that are deposited evenly over the substrate (Fig.-3a). The thin film is free from cracks and holes as the particles are densely packed. However, the SEM image (figure 3b) of 6 at.% cobalt doped manganese oxide thin film shows cracks and holes which can be attributed to the formation of larger size particles through agglomeration at higher temperatures in presence of higher concentrations of cobalt.[26] The particle morphology changes from spherical to rather elongated shape for 6 at.% cobalt doping. The average particle size increases to 70 nm. These results indicate that by increasing the annealing temperature, the crystallinity, and grain size increase at the same time increase in cobalt doping also favours the formation of crystalline particles with an increase in size due to the synergistic effect. The elemental composition of cobalt doped manganese

oxide thin film is examined using the EDS spectrum shown in Fig.-3c. EDS spectrum shows the existence of oxygen, cobalt, and manganese elements with the composition that corresponds to $Co_xMn_{3-x}O_4$.

UV-vis Spectroscopic Studies

A UV-vis spectrometer was used to characterize the optical properties of prepared thin films. There was a maximum absorption of radiation in the wavelength region of 300-400nm that was recorded in the optical absorption spectrum (figure not shown). Thick films that have been heated between 350 and 450 ° C have an absorbance peak of 350 nm, whereas those heated to 550 degrees Celsius have an absorbance peak between 350 and 420 nanometers. The shift in absorption peak location is thought to be due to the annealing and doping of thin films.[27] The freshly prepared thin films' transmittance decreases as the annealing temperature rises. α = 2.303 A/t, where A is optical uptake and t represents layer thickness, is the absorption coefficient obtained from Lambert's law. Surface Emission Microscopy (SEM) is used to measure the film's thickness (200 nm). Figure-4 (A)depicts Tauc's plot of (αhv)2 vs h, which is used to determine the direct band gaps for the thin films.

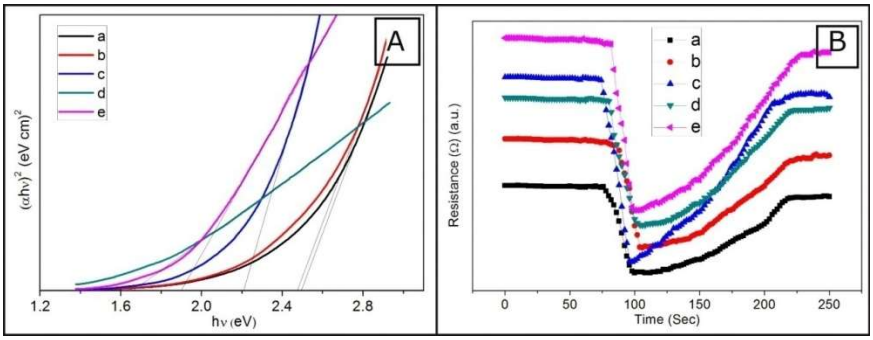

Fig.-4: (A) plots of $(\alpha hv)^2(eV\ cm^{-1})^2$ Vs hν(B) Time dependence of sensing response for 4 at.% cobalt doped manganese oxide thin film annealed at (a) 350 ºC, (b) 450 ºC (c) 550 ºC, (d) 2 at.% cobalt annealed at 550 ºC and e) 6 at.% cobalt annealed at 550 ºC

Extending the linear section of the plot of $(\alpha hv)^2$ versus h to cross with the X axis at α= 0 yields the band gap values. The band gap energy of 4 at.% cobalt doped manganese oxide thin layers annealed at 350, 450, and 550ºC are 2.5, 2.45, and 2.2 eV respectively. Similarly, the band gap energy for the variation of cobalt doping 2 at% and 6 at.% with annealing at 550ºC are 1.65 and 1.9 eV respectively. It is evident from the results that the band gap energy decreases with increasing the annealing temperature and cobalt doping.[28]The higher annealing temperature of thin films favors the formation of crystalline particles whereas the increasing doping induces defects in the crystal which narrow down the band gap.

Sensing Characteristics

The sensing characteristics of the prepared thin films at 250 ºC for 100 ppm of ethanol vapor in dry air were investigated. The results obtained are depicted in Fig.-4B. It is obvious that the thin film shows a response to ethanol vapor with appreciable sensitivity.[29-30] These thin films exhibit rapid response and reach a steady state within 30 seconds of exposure to ethanol vapor. From the shape of the response curve, it is evident that the 4 at% cobalt doped manganese oxide annealed at 550ºC for 2 hrs shows a rapid response among the prepared electrodes for this study and reached a steady state quickly. The resistance of all of the thin film electrodes in the test gradually increases after reaching a steady state, and this may be attributed to the active centers being saturated with the target gas and its products. When subjected to dry air, the resistance of the sensing cobalt doped manganese oxide thin films rises until it approaches its value 0. In general, the response of thin films annealed between 350 and 450ºC is lower. As a consequence, the 4 percent cobalt doped manganese oxide thin film annealed at 550ºC shows a superior response than the 2 and 6 percent cobalt doped manganese oxide thin films. The sensing response increases with increasing the cobalt content and reaches a maximum at 4 at% of cobalt content, beyond that a decrease in response for 6 at.% of cobalt content was observed. These facts can be attributed to the availability of free electrons as well as the morphology of the particles of the thin films. The 4 at.% cobalt doped manganese oxide thin film produced by jet nebulizer spray pyrolysis followed by

annealing at 550°C for 2 hours has the greatest sensitivity to ethanol.[31-34] However, further optimization studies have to be performed to ascertain its potential as a promising candidate material for sensor applications. The sensing process is described by oxygen decomposition and adsorption on the thin film's surface.[35-36]

$$O_{2(g)} \leftrightharpoons O_{2(ads)}$$

$$O_{2(ads)} + e^- \leftrightharpoons O^-_{2(ads)}$$

$$O^-_{2(ads)} + e^- \leftrightharpoons 2O^-_{(ads)}$$

$$O^-_{(ads)} + e^- \leftrightharpoons O^{2-}_{(ads)}$$

The oxygen is chemisorbed on the active sites of the thin films and at the elevated temperature it becomes O_2^-, O^-, and O^{2-}. Though the target vapor, ethanol has a chance to react with any of these forms of oxygen, thermodynamically, it is oxidized as described in equation (3) and releases electrons into the conduction band.

$$C_2H_5OH + 6O^{2-}_{(ads)} \rightarrow 2CO_{2(g)} + 3H_2O + 12e^- \quad (3)$$

CONCLUSION

Manganese oxide thin films generated utilizing the jet nebulizer spray-pyrolysis technique was studied for the effects of temperature and cobalt doping on their properties. The crystallite and particle sizes are dependent on the annealing temperature as well as the dopant cobalt concentration, as seen by Xrd and SEM images. The SEM images show that the jet nebulized spray pyrolysis technique generated densely packed uniform size particles. When the thin film is heated at 550 degrees Celsius, the crystalline quality of the particles improves invariably, but doped cobalt causes the particles to aggregate into larger nano sizes.A narrow band gap with an increase in cobalt content is observed in these films. The ethanol sensitivity of the 4 at. % cobalt doped manganese oxide thin film produced by jet nebulizer spray pyrolysis followed by annealing at 550°C for 2 hours is greater.

ACKNOWLEDGEMENT

The UGC (MRP-5394/14 (SERO/UGC) March 2014) provided crucial support to the authors for material synthesis. The authors used facilities for material analysis and characterization provided by Sri Ramakrishna Mission Vidyalaya College of Arts and Science, Coimbatore, Alagappa University, Karaikudi, India.

REFERENCES

1. G. Guisbiers, S.M. Rosales F.L. Deepak, *Journal of Nanomaterials*, Article ID **180976**, (2012), https://doi.org/10.1155/2012/180976
2. M.S. Chavali, M.P. Nikolova, *SN Applied Sciences*, **1**, 607(2019), https://doi.org/10.1007/s42452-019-0592-3
3. S.P. David, A. Soosaimanickam, T. Sakthivel, B. Sambandam, A. Sivaramalingam, *Environmental Chemistry for a Sustainable World*, **55**, 185(2021), https://doi.org/10.1007/978-3-030-53065-5_6
4. I. Sandu, L. Presmanes, P. Alphonse, P. Tailhades, *Thin Solid Films*, **495(1–2)**, 130(2006), https://doi.org/10.1016/j.tsf.2005.08.318
5. T. Guo, M.S. Yao, Y.H. Lin, C.W. Nan, CrystEngComm, **17**, 3551(2015), https://doi.org/10.1039/C5CE00034C
6. S.G. Sayyed,A.V. Shaikh, D.P. Dubal, H.M. Pathan, *ES Energy & Environment*,**14,** (2021), https://doi.org/10.30919/esee8c522
7. L. Jayaselvan, S.T. Rajan, C.G. Sambandam, *Rasayan Journal of Chemistry*, **13(4)**, 2223(2020).
8. S. Thirumalairajan, K. Girija, M. Sudha, P. Maadeswaran, J. Chandrasekaran, *Journal of Optoelectronics and Advanced Materials*, **2**, 779(2008).
9. R. Peng, N. Wu, Y. Zheng, Y. Huang, Y. Luo, P. Yu, L. Zhuang, *ACS Applled Materials & Interfaces*, **8 (13)**, 8474(2016), https://doi.org/10.1021/acsami.6b00404
10. T.L. Le, S.G. Fritsch, P. Dufour, C. Tenailleau, *Thin Solid Films*, **612**, 14(2016), https://doi.org/10.1016/j.tsf.2016.05.030
11. D. Yang, *Journal of Power Sources*, **198**, 416(2012), https://doi.org/10.1016/j.jpowsour.2011.10.008

12. M.A. Dahamni, M. Ghamnia, S.E. Naceri, C. Fauquet, D. Tonneau, J.J Pireaux, A Bouadi, *Coatings*,**11(5)**, 598(2021), https://doi.org/10.3390/coatings11050598
13. H. Li, D. Chen, S. Li, C. Kang, Q. Liu, *Ionics,* **27**, 2181(2021), https://doi.org/10.1007/s11581-021-03957-7
14. P.A. Shinde, N.R. Chodankar, S. Lee, E. Jung, S. Aftab, Y.K. Han, S.C. Jun, *Chemical Engineering Journal*, **405**, 127029(2021), https://doi.org/10.1016/j.cej.2020.127029
15. N. Sethupathi, P. Thirunavukkarasu, V.S. Vidhya, R. Thangamuthu, G.V.M. Kiruthika, K. Perumal, H.C. Bajaj, M. Jayachandran, *Journal of Materials Science: Materials in Electronics*, **23**, 1087(2012), https://doi.org/10.1007/s10854-011-0553-0
16. D. Yang, *Journal of Power Sources*, **198**, 416(2012), https://doi.org/10.1016/j.jpowsour.2011.10.008
17. S. Mourdikoudis, R.M. Pallares, N.T.K. Thanh, *Nanoscale*, **10**, 12871(2018), https://doi.org/10.1039/C8NR02278J
18. N.M. Deraz, A.A. Abdeltawab, S.S. Al-Deyab, *Asian Journal of Chemistry*, **26(7)**, 2120(2014), http://dx.doi.org/10.14233/ajchem.2014.16521
19. O. Bayram, E. İgman, H. Guney, O. Simsek, *Superlattices and Microstructures*, **128**, 212(2019), https://doi.org/10.1016/j.spmi.2019.01.025
20. S. Rani, S.C. Roy, N. Karar, M.C. Bhatnagar, *Solid State Communications*, **141(4)**, 214(2007), https://doi.org/10.1016/j.ssc.2006.10.036
21. D. Berger, A.P. de Moura, L.H. Oliveira, W.B. Bastos, F.A. La Porta, I.L.V. Rosa, M.S. Li, S.M. Tebcherani, E. Longo, J.A. Varela, *Ceramics International*, **42(12)**, 13555(2016), https://doi.org/10.1016/j.ceramint.2016.05.148
22. B. Allabergenov, U. Shaislamov, H. Shim, M.J. Lee, A. Matnazarov, B. Choi, *Optical Materials Express*, **7(2)**, 494(2017), https://doi.org/10.1364/OME.7.000494
23. Y. Cong, B. Li, S. Yue, D. Fan, X.j. Wang, *The Journal of Physical Chemistry C*, **113(31)**, 13974(2009), https://doi.org/10.1021/jp8103497
24. V.N. Suryawanshi, A.S. Varpe, M.D. Deshpande, *Thin Solid Films*, **645**, 87(2018), https://doi.org/10.1016/j.tsf.2017.10.016
25. R.C. Massé, C. Liu, Y. Li, L. Mai, G. Cao, *National Science Review*, **4(1)**, 26(2017), https://doi.org/10.1093/nsr/nww093
26. M. Kusuma, G.T. Chandrappa, *Journal of Science:Advanced Materials and Devices*, **4 (1)**, 150(2019), https://doi.org/10.1016/j.jsamd.2019.02.003
27. M.A. Sayeed, H.K. Rouf, K.M.A. Hussain, *Materials Research Express*, **8**, 086401(2021).
28. M. Sayed, A. Arooj, N.S. Shah, J.A. Khan, L.A. Shah, F. Rehman, H. Arandiyan, A.M. Khan, A.R. Khan, *Journal of Molecular Liquids*, **272**, 403(2018), https://doi.org/10.1016/j.molliq.2018.09.102
29. I.E. Abdurakhmanov, O.A. Kuchkarov, E. Abdurakhmanov, *Rasayan Journal of Chemistry*, **13(3)**, 1486(2020).
30. D. A. Oliveira, J. L. Lutkenhaus, J.R. Siqueira, *Thin Solid Films*, **718**, 138483(2021), https://doi.org/10.1016/j.tsf.2020.138483
31. E.A. Kirupa, A.M.E. Raj, C. Ravidhas, *Journal of Materials Science: Materials in Electronics*, **27(5)**, 4810(2016), https://doi.org/10.1007/s10854-016-4362-3
32. C. Liu, S. Navale, Z.B. Yang, M. Galluzzi, V. Patil, P.J. Cao, R. Mane, F. Stadler, *Journal of Alloys and Compounds*, **727**, (2017), https://doi.org/10.1016/j.jallcom.2017.08.150
33. L.B. Said, A. Inoubli, B. Bouricha, M. Amlouk, *Spectrochimica Acta, Part A:MolecularandBiomolecular Spectroscopy*, **171**, 487(2017), http://dx.doi.org/10.1016/j.saa.2016.08.014
34. M.A. Amara, T. Larbi, A. Labidi, M. Karyaoui, B. Ouni, M. Amlouk, *Materials Research Bulletin*, **75**, 217(2016), https://doi.org/10.1016/j.materresbull.2015.11.042
35. S.M. Kanan, O.M. El-Kadri, I.A. Abu-Yousef, M.C. Kanan, *Sensors*, **9(10)**, 8158(2009), https://doi.org/10.3390/s91008158
36. J. Bartolomé, M. Taeño, R. Martínez-Casado, D. Maestre, A. Cremades, *Applied Surface Science*, **579**, 152134(2022), https://doi.org/10.1016/j.apsusc.2021.152134

[RJC-7009/2022]